Investigation of Flow Pattern and Pressure Loss of A V94.2.5 Gas Turbine Air Intake System Using 3D Numerical Modeling

KHASHAYAR KHORSAND, S. M. H. KARIMIAN*,M.Varmaziar, S.SARJAMI,

Department of Engineering,Professor*,Department of Aerospace Amir Kabir University*

Mapna Turbine Engineering and Manufacturing Company (TUGA)

231 Mirdamad Ave. Tehran - I.R.Iran; P.O.BOX15875-5643

* Khorsand.khashayar@mapnaturbine.com
kh.khorsand@gmail.com
www.mapnaturbine.com

Abstract—Air intake system of a 160 MW gas turbine cycle has been modeled and analyzed using numerical simulation in a full 3D perspective. Analysis was carried out using the commercial numerical simulation software, FLUENT 6.3. Inputs and Boundary condition gathered from the design working condition of a Siemens V94.2 gas turbine, installed in the Khoramshahr power plant. This paper deals with flow pattern simulation in order to improve the pressure loss and flow characteristic of the gas turbine compressor inlet. The understanding developed with reference to recirculation flows and non-uniform flow over the whole air intake system, provides valuable insights to designers for optimization of components for better efficiency.

Key-words: - Gas turbine; Air intake; Numerical Simulation; Flow Pattern; Pressure Loss

1. Introduction

Air intake is an important part of a power plant gas turbine because of the high pressure drop will leads to turbine gross power output drop. For example, 1” wg reduction is equal to 0.355% power output gain and for V94.2 type turbine with the output power of 160MW this pressure loss is equal to 0.568MW so that Over a 4 month period of use at $0.10/kWh, Revenue will increase to $160000 [1]. Due to the high complexity of the flow pass in the air intake system, it is vital to investigate the flow passage and air flow characteristic such as static pressure, velocity and also force exerted to the structure by the momentum change. Moreover, the local pressure losses (local resistance) are caused by the fluid flow through the duct fittings, pre-filter, anti icing system, after filter, bending duct, transient section and inlet cone which change the direction of the flow or affect the flow in the straight duct with variable cross-section. The use of simulation made it possible to work together to propose possible design changes that had the potential to reduce the turbulence. The local pressure loss coefficient x for particular duct fitting can be determined purely by experiment and the data can be Since the experimental measurement of the local pressure loss coefficient on the real ductwork which is expensive and time-consuming and also the flow pattern can only be simulated by means of CFD so that it is possible to use advantages of the computer simulation modeling in CFD (computer fluid dynamics) software. The behavior of turbulent air flow motion in computational domain is obtained through CFD/CAD software packages. The understanding developed with reference to recirculation flows in the inlet duct, non-uniform flow around air pass and unequal flow at exit, provides valuable insights to designers for optimization of components for better efficiency [2].

2. Problem description

The air intake has the scope of filtering the combustion air of Gas Turbine Siemens V94.2 and to convoy it to the gas turbine compressor.

It has also the main function of silencing the noise from the compressor to the surrounding and to the air inlet. Ancillary functions are also performed by some subsystems which are:

- Anti-icing system to avoid ice formation
- Pulse jet system for cleaning filters
- Damper for segregating the compressor area
- Maintenance area with hoist for filter

Air with flow rate of 518 $^{kg}/_{s}$ at base load design condition is penetrating upward/horizontally through a bird screen and an insect screen which is mounted at the mouth of the weather hoods and is entering at a level between 10 and 22 m above ground level, so there is first separation of biggest particles. (Fig.1). Air is penetrating upward/horizontally through a bird screen and an insect screen which are mounted at the mouth of the weather hoods. After the anti-icing diffusers there is the inertial sand trap grid which has the function of retaining the coarse sand particles especially during sand storms. It is constituted of vertical blades shaped, disposed in opposite in order to force the air stream to sharp elbows, and consequently to loss the suspended heaviest particles by means of the inertia effect. After then there are the main filters, in number of 1200 cylindrical cartridges. The cleaned air is now entering in the transition piece. Then the outside air can enter directly through these doors and the filter house avoids the risk of imploding. After the transition piece there is the silencer Panels are vertically removable through the roof. The lower part of the duct has the function of convoying air into the gas turbine compressor. An inner cone is attached to the turbine body to avoid turbulence as much as possible: inside this cone it is positioned the shaft connecting turbine to generator.

The geometry and dimensions are based on the Khoramshahr Power plant units and the physical properties of air intake and required data related to the flow are in coincidence with the design point of this power plant site at south west of Iran.

In order to modeling of the system shown in the Fig.1, the components divided to the parts and modeled in GAMBIT 2.2 in 3D and has been meshed using unstructured and combined multi block structured mesh.

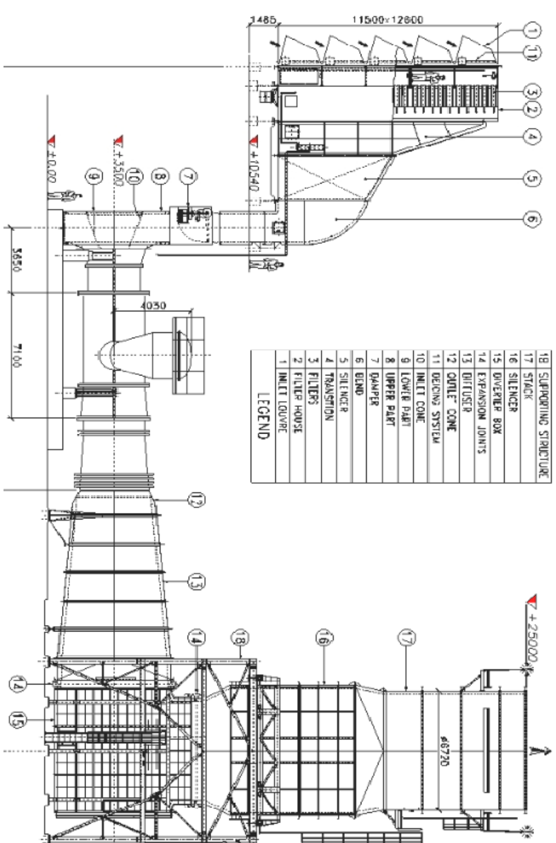

Figure 1. Siemns V.94.2.5 Khoramshahr gas turbine Air intak system

Figure 2: Khoramshahr power plant V94.2.5 Gas Turbine air intake units

3. *governing equation (continuity, momentum and energy equation)*

Since air flow velocity is lower than the so-called compressibility Mach number 0.3, the effect of fluid compressibility was not considered so that the following preconceptions were considered in the analysis;

- Governing equations consisted of 3-dimentional steady state Navier-Stokes equations
- There is no energy source and the working temperature is the ISO design condition at the site. All the fluid thermal properties were considered constant corresponding to the working temperature of 30 degree Celsius. In addition the state condition of ideal gas was used to calculate the air density and viscosity.
- Turbulence modeling was carried out via Standard $k-e$ model.
- Navier-Stokes equations was considered in FULL 3 Dimensional so the energy and momentum equation is considered as the following:

$$\frac{\partial}{\partial x_i}(r u_i) = 0 \tag{1}$$

$$\frac{\partial}{\partial x_j}(r u_i u_j) = -\frac{\partial P}{\partial x_i} + \frac{\partial}{\partial x_j}[m(\frac{\partial u_i}{\partial x_j} + \frac{\partial u_j}{\partial x_i} - \frac{2}{3} d_{ij} \frac{\partial u_k}{\partial x_k}) - r \overline{u_i' u_j'}] \tag{2}$$

$$i = \begin{cases} 1 & x-direction \\ 2 & y-direction \\ 3 & z-direction \end{cases}$$

4. *Boundary condition*

In connection with the flow pattern in 5 story of the air intake system, only has it been considered one story for flow insulation in the first part of the air intake simulation and the mass flow rate of air has been considered as the base load of 103.6 $\frac{kg}{s}$.

The inlet boundary condition is set as follow:

ISO air property design condition at the site:(

T_1=15℃, P_1=1bar, $\dot{m}_1 = 518 Kg/s$, ρ_1=1.22522Kg/m^3, μ_1=17.8912×10^{-6}Kg/m.s,

Hydraulic diameter of the air intake system

$$d_h = \frac{4 \times a}{P} \quad (3)$$

$$d_{h,1} = \frac{4a_1}{P_1} = \frac{4 \times 22.03798}{28.3546} = 3.1089m$$

Hence the air Reynolds number is

$$Re = \frac{(\rho \times V) \times d_h}{\mu} = \frac{\left(\dot{m}/a_1\right) \times d_h}{\mu} \quad (4)$$

$$Re_1 = \frac{\frac{518}{5} \times 3.1089}{22.03798 \times 17.8912 \times 10^{-6}} = 8.17 \times 10^5$$

Where a_1 denotes area of one-fifth of the air intake system and P_1 represents the premeter of above mentionedportion of air intake system. Air turblance intensity was chosen according to [4]:

$$T.I = 0.16 \times Re^{-1/8} \quad (5)$$

$$T.I_1 = 0.16 \times Re_1^{-1/8} = 0.16 \times (8.17 \times 10^5)^{-1/8} = 2.9\%$$

And used in proper part of Fluent 6.3 simulation GUI.

5. turbulence modeling

The $k - e$ standard model has been utilized in order to model the turbulence of the flow. K refers to turbulent Kinetic energy and the term 'e' refers to turbulent energy dissipation rate. Among all two-equation Turbulence models that have been presented so far, the model proposed by Launder and Spalding is the most well-known, $k - e$ standard model. In this model, the turbulent viscosity is calculated as following:

6. Numerical approach

In order to numerically simulate the flow field within the domain, the commercial FLUENT 6.3 software was used based on the control-volume approach. The equations of scalar variables were discredited by QUICK scheme which has a good result compare to the other method especially in non-straight flow.

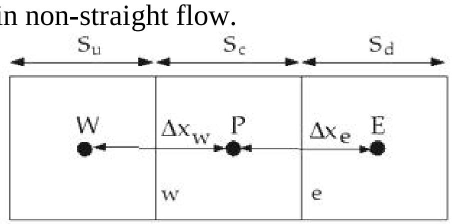

Figure 3: QUICK model Discrimination schematic diagram

Contemporary QUICK scheme is based on the following equation:

$$f_e = q\left[\frac{S_d}{S_c + S_d} f_P + \frac{S_c}{S_c + S_d} f_E\right] + (1-q)\left[\frac{S_u + 2S_c}{S_u + S_c} f_P - \frac{S_c}{S_u + S_c} f_W\right] \quad (6)$$

Where E and W refer to East and west cells respectively[3]. As we can seen for θ=1the equation 6 turns to central interpolation and for θ=0 this will be upwind second order considering the fact that in the present simulation it has been used θ=1/8.

For pressure interpolation in control volume surface, PRESTO method was implemented due to the high precision in modeling of flow in curvature passes and For handling the pressure-velocity coupling SIMPLE algorithm was implemented. It should be noted that there were some serious convergence problems. In order to get to reliable Results, we started from lower inlet mass flow rates and then increase it step by step. Every time the Convergence was obtained in a specified mass flow rate, before increasing the mass flow rate to a higher Level we switched the equations to time dependent conditions and after getting to semi-steady state conditions, we again switched to steady state equations.

When the flow around the object is analyzed, experimentally or numerically, taking into account its span wise dimension and length, new phenomena appear, characterized by the presence of stream wise vortices, with non-unique properties and additional nonlinear interactions leading to frequency doubling effects and route to chaos with increasing Reynolds numbers. These effects were initially found experimentally by Williamson (1998a, b, 1989, 1992). They have been confirmed and analyzed in depth in a series of numerical simulations by M. Braza and her coworkers, where the detailed mechanisms of the two modes have been clearly identified (Persillon and Braza (1998) and Braza et al. (2001)) so that it is vital to model the whole air intake system in full 3D due to the sudden change in air passage[5,6].

7. GRID INDEPENDENCY CHECK

In order to achieve a suitable grid with proper concentration, selected geometry was meshed using 4 different sets of grid with different concentration. The grid independency was checked out using the air intake parts According to figure 2, the grid with 362088,475179 , 592032and 700690 cells provided the results independent from grid concentration, in the other words, finer mesh did not have any effect on results accuracy.

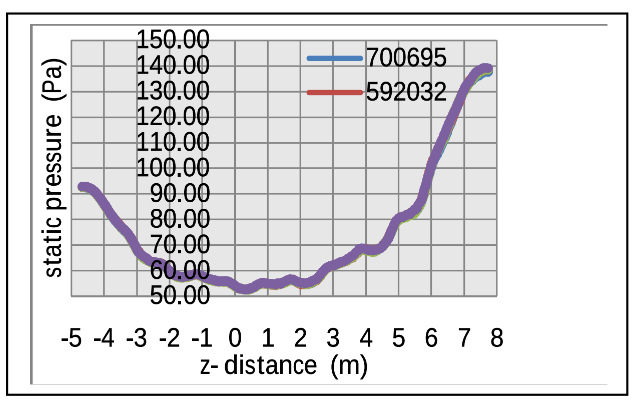

8. Flow pattern, velocity profile, pressure drop and force exerted to the structure of air intake system

The aim of these simulations was mainly to investigate the flow pattern in the air intake system that most appropriately fit the idea of eliminating vortices and reducing the intensity of turbulence in the flow field. The whole system is divided into subpart in order to convenience in analysis and has been modeled with 4245795 cells in a combination of structured and unstructured mesh as shown in the figure 5. According to the figure3, shows the total pressure loss of the second and the third part is approximately as 1391 Pa. with standing the fact that the inertial filters and anti icing pressure loss did not take into account and about 75% of the loss (1056 pa) belongs to the main filters.

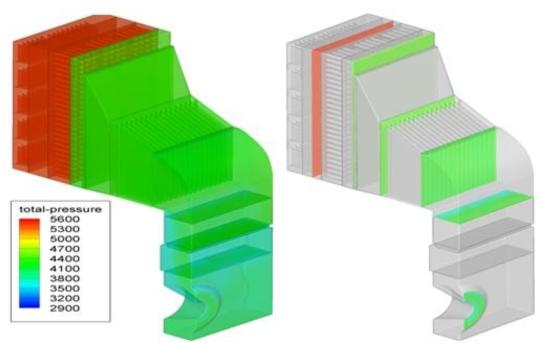

Air intake internal cross section	Total guage pressure cells 4245797	Total guage pressure cells 3231779	error
1	5430	5473	0.80 %
2	4373	4416	0.97 %
3	4373	4415	0.97 %
4	4313	4355	0.97 %
5	4072	4122	1.22 %
6	4038	4084	1.12 %

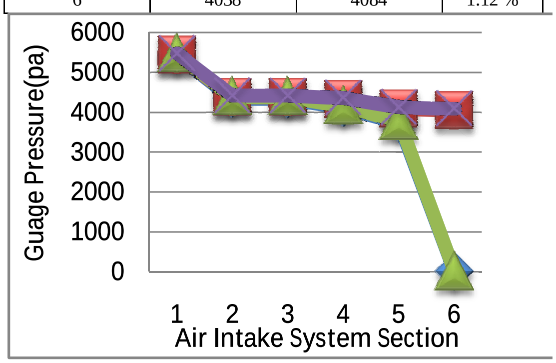

Figure 5: comparison between average static gauge pressure in Pascal (Green) and average total pressure (red) for various air intake cross sections

The system is divided to the subpart and was being simulated as follows:

8.1) Weather hood

After simulation the velocity of air flow has been shown in the figure 6. As it can be seen the air flow enters the weather hood passing from the insect screen and left the hood system to the inertial filters which filter out the dust particles via change of momentum. The vortices have been formed in the left and right part of the weather hood as it can be seen in the figure 7. The plane cross section position is located on the 7.5 meter from center part of the weather hood. Large vortices has been already formed but in the z=5.5 meter the vortices has been eliminated and the flow pattern is almost straight.

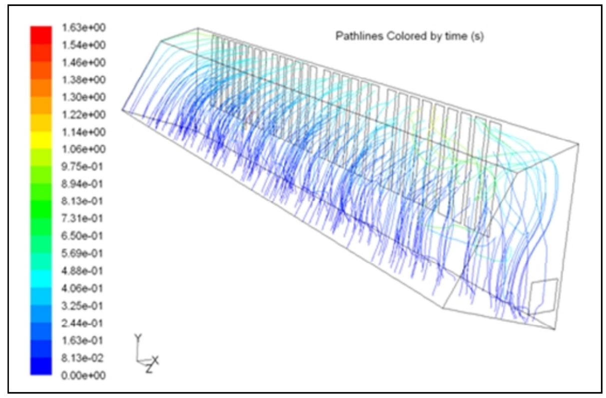

Figure 6. Siemens v94.2 gas turbine air intake weather

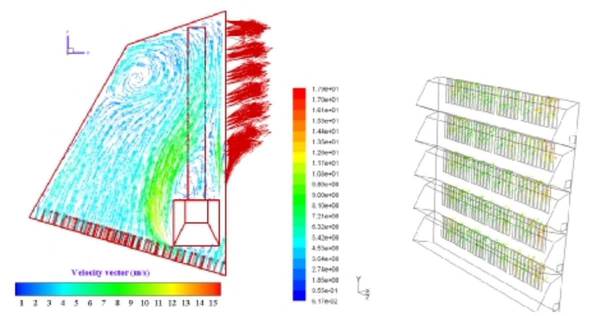

Figure 7. Air intake weather hood simulation in z=7.5 meter

8.2) Filter house

The overall pressure contour in the figure 8 represents the large amount of pressure drop is taken place at the duct corners. Also this may have some consequences such as unsuitable flow separation at the back of the inertial filters. This is May as a consequence of depression in the filter back pressure which may be the root cause of vortices in this area and poor capability of pulse jet filter cleaning of the Khoramshahr Power plant. The geometry of system is complicated with lots of round and sharp edges so that the unstructured tetrahedron mesh was used.

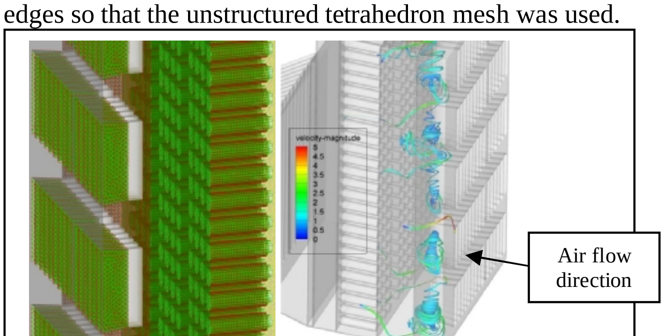

Figure **8**. Filter house simulation mesh generation in gambit (left) and 3D vortices and stagnation points in the void part of the filter house has been already formed.

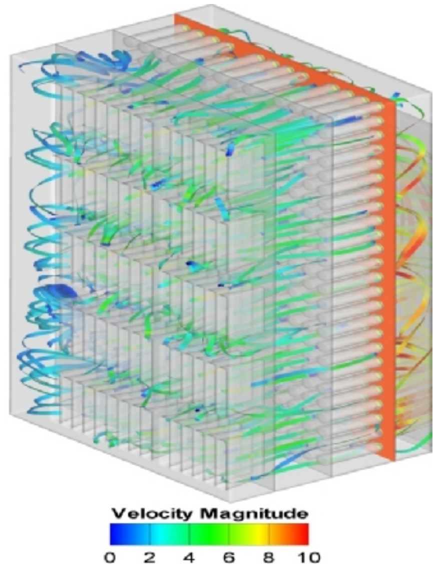

Figure **9**. Simulated velocity magnitude and air streamlines for filter house (left: inertial filters and right it can be seen high efficiency synthetic filters)

8.3) Bending duct and silencers

The third part of the air intake system has been shown in the Figure 10. And it consists of bending duct and silencer- splitters. Calculated static pressure from Figure 10 depict that from the iso cutting plane and due to the increase in velocity magnitude between silencers, the static pressure has been decreased. After simulation and in order to visualize the air pass throw turbine compressor (figure 11), it has been seen that huge vortices has been already formed due to flow separation of the silencers. We came up the idea of improving the geometry and location of the silencers to minimize the pressure loss due to tornado like flow of air in this region which also the silencers sound attenuation performance also will be taken into account in the redesign phase of the project.

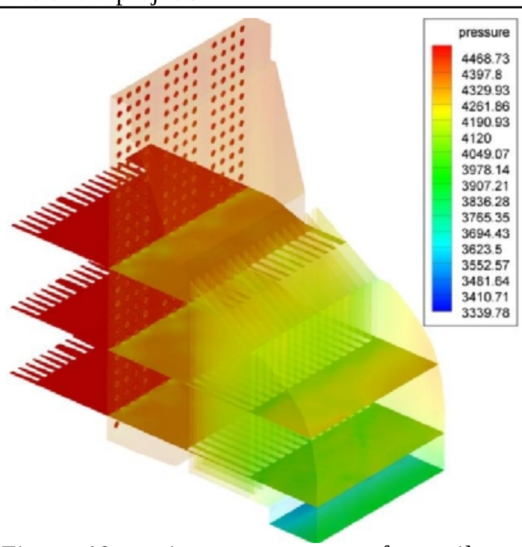

Figure **10**: static gauge pressure from silencer and bending duct part of the air intake system with cutting plane

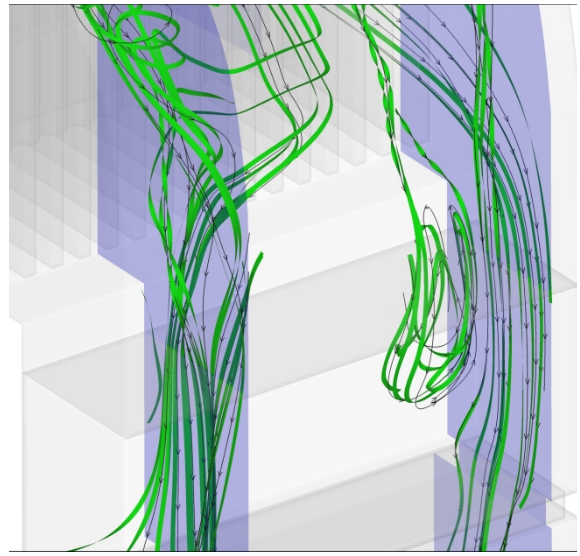

Figure 11: streamline after silencer and bending duct portion of the air intake

8.4) Transition piece and compressor inlet cone

This part is the final part of the whole air intake system which was modeled by unstructured tetrahedron cell for inlet cone and structured cell for transition duct. The simulation has been carried out using the reference pressures of the inlet cone exit area is equal to zero gauge pressure and the site local design pressure have to add to this gauge to become absolute calculated pressure.

The whole air intake system air velocity magnitude is shown in the figure 13 and we can see the zero velocity zones in the lower left part of the inlet cone enclosure which have to be modified as round shape to avoid swirl and pressure loss.

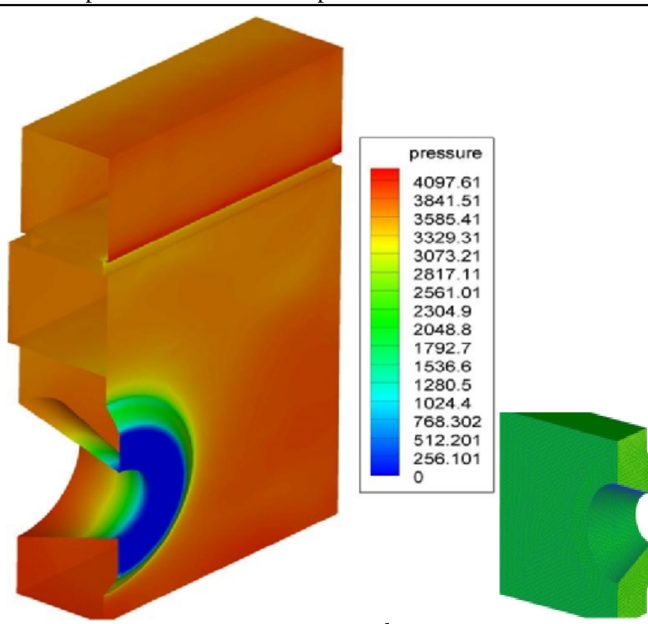

Figure **12**: static gauge pressure from transition piece and inlet cone (left) and inlet cone grid generated (right)

ISSN: 1790-5095

ISBN: 978-960-474-158-8

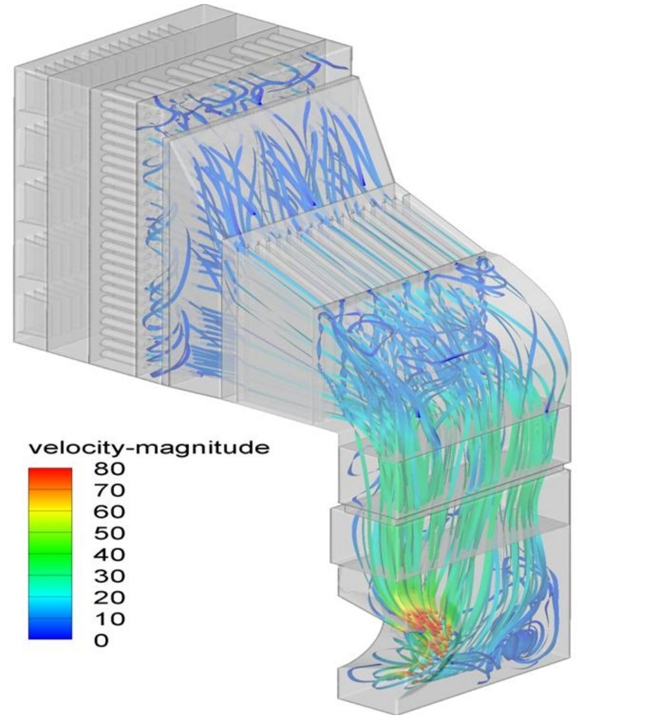

Figure 11 Span wise undulation of the main vortex rows of filters in filter house and stream wise vortices at Re=12.1*10E5

9.) conclusion

The purpose of this research is to investigation of pressure loss and flow specification of air intake system of Khoramshahr Siemens v94.2.5 type gas turbine power plant. In this research, firstly the whole air intake system was modeled in Gambit2.2 software. 3D simulation of air intake system using FLUENT 6.3 software to investigate the pressure drops in order to understanding the flow pattern in air intake compartment and the future optimization was carried out. It should be noted that three dimensional modeling involves all the details of the considered System except the pressure loss due to the silencer grid part along with the sound and air pressure interaction. Also, since there was not any experimental data in fingertips, verification of the results obtained by numerical simulation could not be performed, therefore these results could be as an estimation of what occurs in the air intake system for further optimization in design.

NOMENCLATURE

ρ Gas density (kg/m^3)
u horizontal component of velocity vector (m/s)
v vertical component of velocity vector (m/s)
P Pressure (Pa)
k Turbulent kinetic energy production rate
ε Turbulent kinetic energy dissipation rate
c_p Specific heat (J/kgK)
φ general dependent variable

ACKNOWLEDGMENT

The authors wish to thank the financial support of the MAPNA group and TUGA executive management to provide writers with the opportunity to perform the research.

REFERENCES

[1] Gas Turbine Inlet Anti-Icing system cataluge ,www.higg-kane-atco.com

[2] Chen, J., Haynes, B. S., Fletcher, D. F., 1999, “A Numerical and Experimental Study of Tangentially Injected Swirling Pipe Flows,” Second Int Conference on CFD in the Minerals and Process Industries, CSIRO, Melbourne, Australia.

[3] H K Versteeg, W Malalasekera. An introduction to computational fluid dynamics, the finite volume method. s.l. : Pearson Education Limited, 2007.

[4] Braza, M., Faghani, D., Persillon, H. (2001). Successive stages and the role of natural

[5] vortex dislocations in three-dimensional wake transition.*J. Fluid Mech.*, 439, 1–41.

[6] White, Frank M. Fluid mechanics. s.l. : McGraw-Hill, 2003.

[7] Numerical simulation of turbulent flow in complex geometries used in power plants; C. Bhasker;2001

[8] J.Blazek. Computational fluid dynamics, Principles and applications. s.l. : Elsevier Ltd, 2005.

[9] Leonard, B.P. and Mokhtari S., 1990, “ULTRA-SHARP Nonoscillatory Convection Schemes for High-Speed Steady Multidimensional Flow.” NASA TM 1-2568 (ICOMP-90-12), NASA Lewis Research Center.

[10] computer methods in applied mechanics and engineering. 1974.

[11] The numerical computation of turbulent flows. B.E. Launder, D.B. Spalding.

[12] Fluent 6.3 User's Guide 2006.